Electromagnetic Axisymmetric Analysis of Monopole Antenna Over a Perfectly Electric Ground Plane by a Meshless Local Petrov-Galerkin Method

Ramon Dornelas Soares
Postgraduate Program in Electrical Engineering
Federal University of Minas Gerais
Av. Antonio Carlos 6627, 31270-901
Belo Horizonte, MG, Brazil
Email: ramon_dornelas@yahoo.com.br

Renato Cardoso Mesquita
Dept. Electrical Engineering
Federal University of Minas Gerais
Av. Antonio Carlos 6627, 31270-901
Belo Horizonte, MG, Brazil
Email: renato@ufmg.br

Fernando J. S. Moreira
Dept. Electronics Engineering
Federal University of Minas Gerais
Av. Antonio Carlos 6627, 31270-901
Belo Horizonte, MG, Brazil
Email: fernandomoreira@ufmg.br

***Abstract*—This work describes a meshless method to obtain the electromagnetic characteristics of a monopole placed over a perfectly electric ground plane. The Meshless Local Petrov-Galerkin is used with shape functions generated by Moving Least Squares. Boundary conditions are imposed by a collocation method that does not require any numerical integration. The proposed axisymmetric analysis has a simple implementation and reduced computational effort. The results are in agreement with theoretical data and simulations found in the literature.**

I. Introduction

Monopole antennas have been vastly used due to its simple structure and attractive characteristics. Airborne and ground based systems are some of the most common applications [1]. Several specific applications can also be listed, where the antenna is partially submerged in non-homogeneous environments like oil and water [2], or involved by different mediums as in the coated monopole antenna [3], [4].

In [4], the effects of cavities on monopoles are determined using integral equations solved by the Method of Moments (MoM), which is known to yield accurate results but with a costly computational effort [2]. The Finite Element Method (FEM) was used in [3] and [5]. The simulations are precise, but FEM needs a mesh with several constraints for its construction. Modal expansion techniques are used in [1], [2] and [4]. These works use models with a perfectly conductor plane above the antenna and parallel to ground plane, therefore their antenna analyses can be influenced by the waves reflected by it. Precise results are found due to the particular characteristics of used antenna (that have the main radiation in horizontal direction) and the far position of the perfectly conductor plane.

Meshless methods have been used in mechanic, hydrodynamic, and recently, in electromagnetic area [6]-[14]. Several meshless methods are reported in literature, which can be classified in two categories: the methods based on strong forms and the ones based on weak forms. Methods based on strong formulations use collocation techniques to directly discretize the governing partial differential equations (PDE). These methods have a simple implementation and are computationally efficient. The collocation techniques are generally implemented using radial basis functions [9], [10], [11] or Smoothed Particle Hydrodynamics for Electromagnetics (SPEM) formulations [12].

In weak-form methods, the PDE are converted in a weak formulation using a residual method, and afterward it is discretized with Galerkin or Petrov-Galerkin method. Element Free Galerkin Method (EFGM) uses a global weak-formulation and has been successfully applied in the solution of wave scattering problems [13]. This method requires a background mesh to perform the numerical integration, and so it is not considered a truly meshless method. The Meshless Local Petrov-Galerkin (MLPG) method, used in this work, does not require any mesh and has a local weak-formulation, resulting in sparse matrices minimizing the computational effort. MLPG has been used to solve wave propagation [8], [14] and 3D static problems [7].

The MLPG analysis proposed in this paper, differently from [7], [8] and [14], uses axisymmetric formulations, as in [3] and [5], generating a 2D formulation. Also, it is a weak form method and has advantages when compared to collocation methods in regard to the results precision and numerical stability [15]. The present work extends a previous research [6], where the resonant frequencies and field distribution of axisymmetric cavities were evaluated. Herein, a monopole antenna over a perfectly electric ground plane is analyzed. The axisymmetric monopole model is shown in Fig. 1, which presents the antenna length h and its radius a. The inner and outer coaxial radii are a and b, respectively. Figure 1 also presents the boundaries of the MPLG model, where $\partial\Omega_c$ denotes the surface of perfectly electric conductor, $\partial\Omega_0$ denotes the symmetry axis ($\rho = 0$), $\partial\Omega_r$ denotes the radiation boundary, and $\partial\Omega_f$ denotes the feed region. The union of all these boundaries are represented by $\partial\Omega$ (see Fig. 2).

978-1-4577-1664-5/11/$26.00 ©2011 IEEE

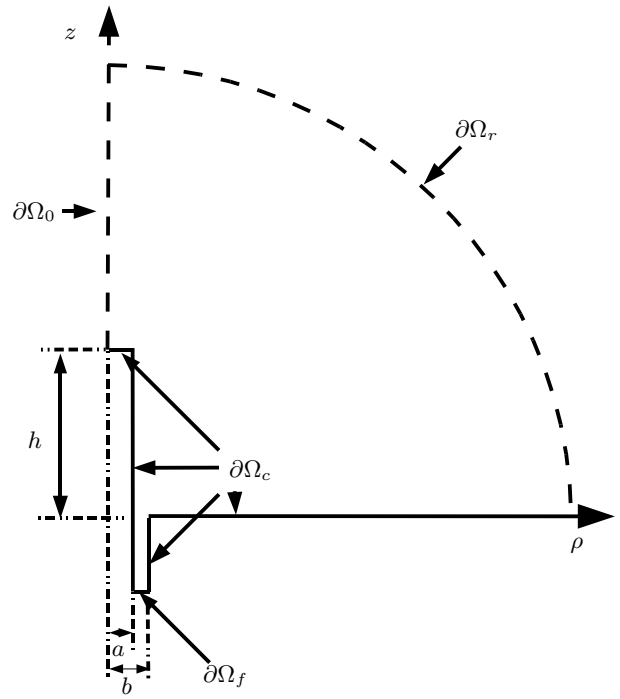

Fig. 1. The axisymmetric monopole model and the MLPG boundaries.

In this work, we present the problem formulation, from which the weak form is derived. The MLPG analysis, its local weak formulation, and its discretized expressions are presented and the numerical analyses of a monopole antenna (see Fig. 1) is shown and discussed.

II. Problem Formulation

The vectorial Helmholtz equation for a source-free region of space containing a material characterized by its relative permittivity ϵ_r and permeability μ_r is given by [16]

$$\nabla \times \left(\frac{1}{\epsilon_r} \nabla \times \vec{H} \right) - k_0^2 \mu_r \vec{H} = 0, \tag{1}$$

where $k_0 = \omega^2 \mu_0 \epsilon_0$ is the free-space wavenumber.

We first make the assumption that material proprieties ϵ_r and μ_r are both independent of ϕ. So, the field distribution is axisymmetric and the magnetic field in (1) has only the ϕ-component and varies only with ρ and z (i.e. $\vec{H} = H_\phi(\rho, z)\hat{\phi}$). This assumption is applied in (1) and results in:

$$\frac{\partial}{\partial \rho}\left[\frac{1}{\rho\epsilon_r}\frac{\partial(\rho H_\phi)}{\partial \rho}\right] + \frac{\partial}{\partial z}\left[\frac{1}{\rho\epsilon_r}\frac{\partial(\rho H_\phi)}{\partial z}\right] + k_0^2 \mu_r H_\phi = 0. \tag{2}$$

The weak form is obtained by the weighted residual method, multiplying (2) by a test function $\psi(\rho, z)$ and integrating it over the problem domain Ω:

$$\iint_\Omega \frac{\partial}{\partial \rho}\left[\frac{1}{\rho\epsilon_r}\frac{\partial(\rho H_\phi)}{\partial \rho}\right]\psi + \frac{\partial}{\partial z}\left[\frac{1}{\rho\epsilon_r}\frac{\partial(\rho H_\phi)}{\partial z}\right]\psi dA + k_0^2 \iint_\Omega \frac{\mu_r}{\rho}(\rho H_\phi)\psi dA = 0. \tag{3}$$

After some mathematical manipulations [16], the weak form is obtained:

$$\oint_{\partial\Omega} \frac{\psi}{\rho\epsilon_r}\frac{\partial(\rho H_\phi)}{\partial n} dl - \iint_\Omega \frac{1}{\rho\epsilon_r}\nabla\psi \cdot \nabla(\rho H_\phi) dA + k_0^2 \iint_\Omega \frac{\mu_r \psi}{\rho}(\rho H_\phi) dA = 0. \tag{4}$$

III. The Meshless Approach

In order to numerically solve (4) and determine the unknown variable ρH_ϕ (here, represented by function u), a meshless approach is adopted. This approach begins by spreading nodes (field nodes) inside the problem domain Ω (interior nodes) and at its boundary $\partial\Omega$ (boundary nodes), as shown in Fig. 2. Every node has its coordinates defined by $\mathrm{x_I} = [\rho, \mathrm{z}]$ and has an associated shape function φ_I, which presents values different from zero only in a small region near the node I. This region is known as node's I influence domains, Ω_{F_I} (see Fig. 1). The local approximation of u at a point x is given by

$$u(\mathrm{x}) = \sum_{\mathrm{I}=1}^{\mathrm{N}} \varphi_\mathrm{I}(\mathrm{x}) \mathrm{u_I}\ , \tag{5}$$

where $I = 1, \ldots, N$ are the nodes whose influence domains include point x (defined by $\mathrm{x} = [\rho, \mathrm{z}]^\mathrm{T}$), and u_I are the corresponding nodal values. The set of N nodes is known as the support domain Ω_x (see Fig. 2). The numerical construction of shape function φ and their derivatives are performed through the MLS approximation and involves several matrix manipulations, which are detailed in [15]. Figure 3 shows a MLS shape function for a node located at $\mathrm{x}^\mathrm{T} = [0, 0]$ obtained using 25 nodes uniformly spread in Ω. Figure 4 shows a example of derivative shape function, which is the first derivative ($\varphi_{,\rho}$) with respect to ρ.

IV. The MLPG analysis

The function approximation by MLS (5) is applied to approximate ρH_ϕ in (4). The proposed analysis is similar to MLPG4 [17], but it differs in what concerns the imposition of boundary conditions. We follows some ideas found in [7], which adopts a simple technique known as the meshless collocation scheme to deal with the interface conditions. In the MLPG, interior nodes use the test function ψ_I, which acts in a local region near node I (the node's test domain Ω_{S_I}) where the integrations are carried out. In MLPG4, Ω_{S_I} is generally a circle centered at the interior node I and the corresponding test function ψ_I must satisfy the following requirements:

$$\nabla^2 \psi_I = -\delta(\mathrm{x} - \mathrm{x_I}), \qquad \text{a delta function at } \mathrm{x_I}, \tag{6}$$

$$\psi_I = 0, \qquad \text{at a test domain boundary } \partial\Omega_{S_I}. \tag{7}$$

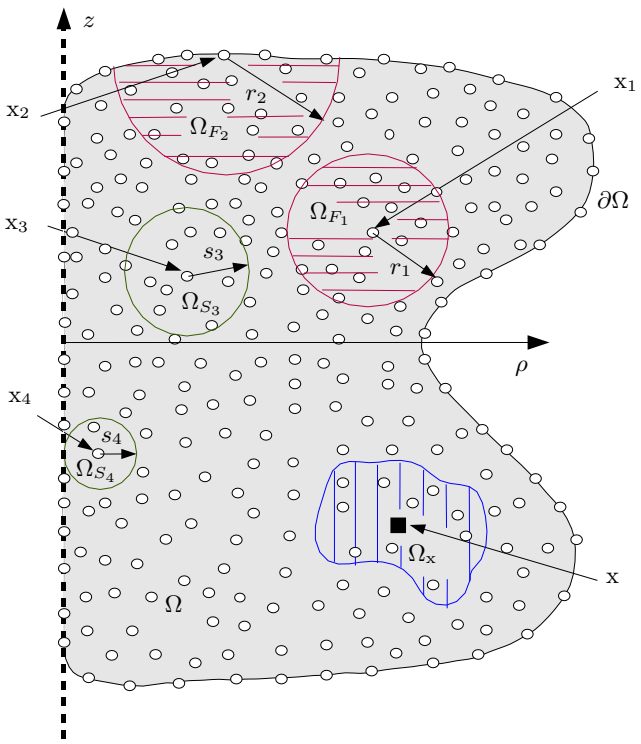

Fig. 2. A computational domain Ω and its boundaries $\partial\Omega$. The horizontal striped regions are the influence domains Ω_{F_1} and Ω_{F_2} of the nodes x_1 and x_2, respectively. The non-striped regions are test domains Ω_{S_3} and Ω_{S_4} of the nodes x_3 and x_4, respectively. The vertical striped region is the support domain Ω_x of a point x.

Conditions (6) and (7) are satisfied by the following test function:

$$\psi_I = \frac{1}{2\pi} \ln\left(\frac{s_I}{|\mathrm{x} - \mathrm{x_I}|}\right), \tag{8}$$

where s_I is the radius of the circular domain Ω_{S_I}, chosen such that Ω_{S_I} does not intersect the global boundary $\partial\Omega$ (see Fig. 2) [7]. The MLPG local weak form can be obtained replacing ψ by ψ_I and ρH_ϕ by u^h in (4), where the boundary integral vanishes due to (7), resulting in:

$$\iint_{\Omega_{S_I}} \frac{\nabla\psi_I \cdot \nabla u^h}{\rho\epsilon_r} dA - k_0^2 \iint_{\Omega_{S_I}} \frac{\mu_r \psi_I u^h}{\rho} dA = 0. \tag{9}$$

This local formulation is versatile; it can be used to analyze a medium with different layers of permittivities or permeabilities (as evaluated in [2] and [3] and [4]). In these cases it is necessary to deal with the discontinuity present in the medium which can be done using the techniques described in [18]. The proposed formulation also can be employed to analyze a monopole placed over a non perfectly electric ground plane. This analyses may be accomplished by using an impedance boundary condition (IBC) when imposing boundary conditions over the metallic surface.

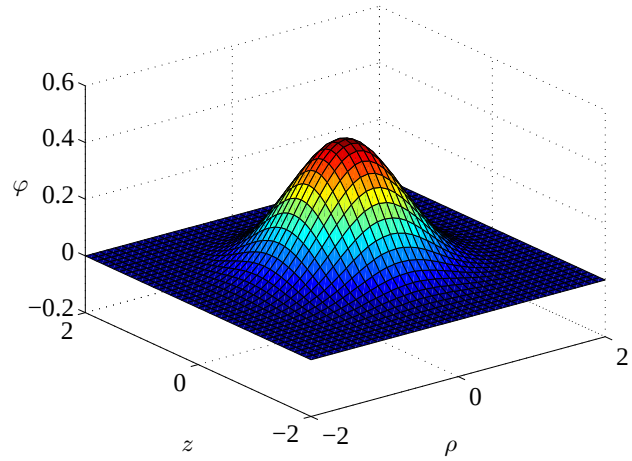

Fig. 3. Shape function φ.

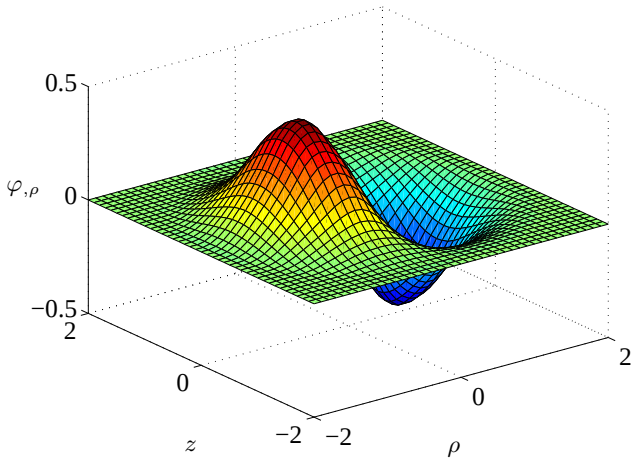

Fig. 4. First derivative of shape function ($\varphi_{,\rho}$) with respect to ρ.

Boundary conditions in $\partial\Omega$ are imposed through the boundary nodes using the meshless collocation scheme that requires no integration [7]. Boundary conditions are expressed in general form as:

$$c(\mathrm{x})u^h(\mathrm{x}) + d(\mathrm{x})\frac{\partial u^h(\mathrm{x})}{\partial n} = f(\mathrm{x}), \tag{10}$$

where $c = 1$ and $d = 0$ if x_I is at a Dirichlet boundary or $c = 0$ and $d = 1$ if it is at a Neumann boundary. f is a known imposed value (i.e. $f(x_I) = 0$ for homogeneous or $f(x_I) \neq 0$ non-homogeneous case). In the monopole geometry (see Fig. 2), the homogeneous Neumann condition must be imposed along the perfect conducting boundary and the field must satisfy homogeneous Dirichlet condition along the axis of symmetry ($\rho = 0$). In addition, we impose in $\partial\Omega_r$ a first-order radiation boundary condition adapted from [16], which can be expressed by specifying $c = jk\rho^{-1}$, $d = \rho^{-1}$, and $f = 0$ in

(11). The excitation at the coaxial waveguide end-wall $\partial\Omega_f$ is imposed by a Dirichlet condition as:

$$\rho H_\phi = \frac{E_0}{\eta} e^{-jk_0 z} \tag{11}$$

where E_0 is the electric field amplitude imposed at $\partial\Omega_f$ (here $E_0 = 1$ V/m) and η is the intrinsic impedance of the coaxial waveguide dielectric (here, $\eta \approx 120\pi\Omega$).

The numerical solution of the problem was obtained by transforming (9) and (10) into a set of linear equations, which results in the following matrix equation:

$$[P]\,[u_I] = [F]\,, \tag{12}$$

where, for interior nodes, the matrix elements are

$$P_{IJ} = \iint_{\Omega_{S_I}} \frac{\nabla\psi_I \cdot \nabla\varphi_J}{\rho\epsilon_r} dA - k_0^2 \iint_{\Omega_{S_I}} \frac{\mu_r \psi_I \varphi_J}{\rho} dA, \tag{13}$$

$$F_I = 0, \tag{14}$$

and, for boundary nodes, they are

$$P_{IJ} = c(\mathrm{x_I})\varphi_\mathrm{J}(\mathrm{x_I}) + d(\mathrm{x_I})\frac{\partial\varphi_\mathrm{J}(\mathrm{x_I})}{\partial \mathrm{n}}, \tag{15}$$

$$F_I = f(\mathrm{x_I}). \tag{16}$$

It can be observed that the P matrix is sparse but asymmetric. The non-zero columns in the I line of the P matrix depend upon all nodes J whose influence domains include the node I (if I is a boundary node) or the evaluation points used to perform numerical integration of Ω_{S_I} (if I is a interior node).

The nodal values u_I can be obtained solving the linear system (12), and afterward they are used to determine ρH_ϕ, at a point x in the domain, as follows:

$$\rho H_\phi(\mathrm{x}) = \sum_{\mathrm{I}=1}^{\mathrm{N}} \varphi_\mathrm{I}(\mathrm{x})\mathrm{u_I}. \tag{17}$$

V. Numerical Results

The monopole antenna (see Fig.1) is analyzed by the proposed technique and compared with models based on a transmission line analogy [19] and with FEM results presented in [3]. Two important antenna characteristics were investigated: the electric current density along the monopole and the input impedance for different monopole lengths.

The current distribution is derived from the obtained field ρH_ϕ along the antenna surface and the boundary conditions for a perfect conductor, $\hat{n} \times \vec{H} = \vec{J}_S$. Figure 5 shows results for the electric current distribution obtained with approximately 4000 nodes, $\partial\Omega_f$ placed at $z = -0.1\lambda_0$, and at 114 MHz. The antenna dimensions are $a = 0.0254\lambda_0$, $b/a = 1.189$, and $h = 0.375\lambda_0$, where λ_0 is the free-space wavelength. The numerical simulation presents an excellent agreement with results found in the literature [19].

The admittance of the monopole was obtained dividing the total electric current at $z = 0$ (ground level) by the interelectrode voltage in the same level, which is determinated integrating the ρ directed electric field through the gap $a - b$ of the antenna model (see Fig. 1). Figure 6 shows the results

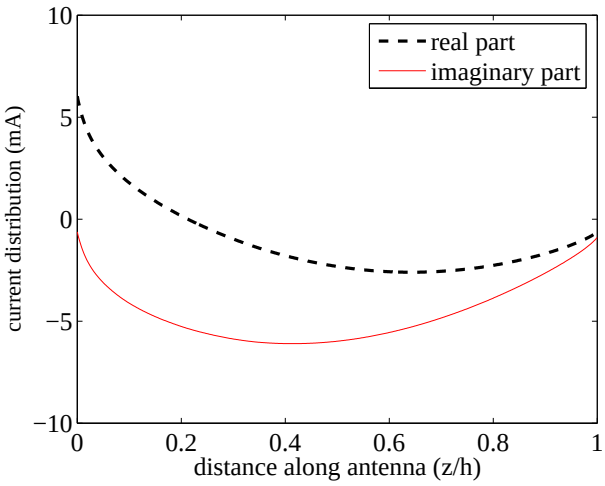

Fig. 5. Current distribution for a monopole over the ground plane.

for the admittance of the monopole as function of its length. The results are in good agreement with [3] and [19].

VI. Conclusion

This work discussed the numerical analysis of a monopole antenna over a perfectly electric ground plane by a Meshless Local Petrov-Galerkin (MLPG) method. The axisymmetric weak formulation is simple and versatile. The proposed MLPG analysis uses collocation method to impose boundary conditions that simplifies the algorithm. The employed method is a local weak form method, which produce sparse matrices and does not require a background mesh.

Two antenna characteristics were numerically evaluated: the superficial current and the admittance. The results are in agreement with theoretical data and simulations found in the literature. The model is easily adaptable to different axially symmetric geometries and can be used to analyze coated monopoles. Implementations with monopoles involved by dielectric materials are being investigated.

Acknowledgment

This work was partially supported by CAPES, CNPq, and FAPEMIG.

References

[1] Z. Shen and R. H. MacPhie, “Sleeve monopole on circular ground Plane”, *International Journal of Modeling: Electronic Network Devices and Fields*, no. 16, pp. 427-441, 2003.

[2] Z. Shen and R. H. Mac Phie, “Modeling of a Monopole Partially Buried in a Grounded Dielectric Substrate by the modal Expansion Method, *IEEE Trans. Antennas and Propagation*, vol. 44, no. 11, 1996.

[3] E. Sumbar, F. E. Steve, and F. S. Chute, “Implementation of Radiation Boundary Conditions in the Finite Element Analysis of Electromagnetic Wave Propagation”, *IEEE Trans. on Microwave Theory and Techniques*, vol. 39, no. 2, 1991.

[4] M. D. Lockard and C. M. Butler, “Effects of Cavities on Monopole Antenna Current Distribution and Decoupling From Mounting Structure”, *IEEE Trans. Antennas and Propagation*, vol. 54, no. 8, 2006.

[5] H. O. Ali and G. Costache, “Finite Element Time-Domain Analysis of Axisymmetrical Radiators”, *IEEE Trans. Antennas and Propagation*, vol. 42, no. 2, 1994.

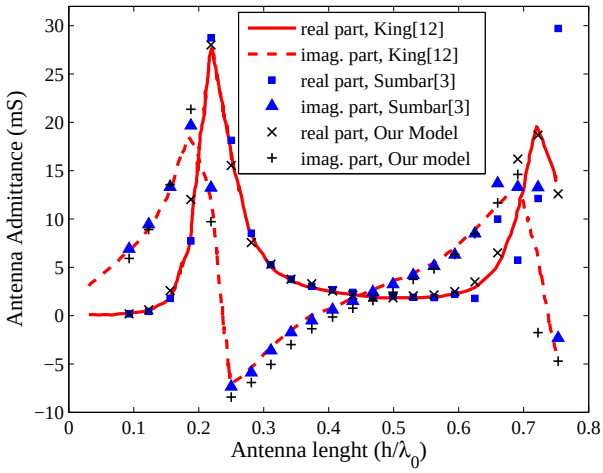

Fig. 6. Admittance versus antenna length for a monopole over the ground plane.

[6] R. D. Soares, R. C. Mesquita, and F. J. S. Moreira, "Axisymmetric Electromagnetic Resonant Cavities Solution by a meshless Local Petrov-Galerkin Method", The 8th International Conference on Computation in Electromagnetics, Wroclaw, pp 176-177, 2011.

[7] W. Nicomendes, R. Mesquita, and F. Moreira, "A meshless local Petrov-Galerkin method for three-dimensional scalar problems", *IEEE Trans. Magnetics*, vol. 47, p. 1214-1217, 2011.

[8] B. Correa, E. Silva, A. Fonseca, D. Oliveira, and R. Mesquita, "Meshless local Petrov-Galerkin in solving microwave guide problems". *IEEE Trans. Magnetics*, vol. 47, p. 1526-1529, 2011.

[9] Y. Tanaka and E. Kunisada,"Study on meshless method using RPIM for transient electromagnetic field", *IEEE Trans. Magnetics*, vol. 47, no. 5, may 2011.

[10] Y. Yu and Z.(David) Chen, "A 3-D radial point interpolation method for meshless time-domain modeling", *IEEE Trans. Microwave Theory and Techniques*, vol. 57, no. 8, August 2009.

[11] T. Kaufmann, C. Fumeaus, C. Engstrom, and R. Vahldieck, "Eigenvalue analysis and longtime stability of resonant structures for meshless radial point interpolation method in time domain", *IEEE Trans. Microwave Theory and Techniques*, vol. 58, no. 12, December 2010.

[12] G. Ala, E. Francomano, A. Tortorici, E. Toscano, and F. Viola, "A smoothed particle interpolation scheme for transient electromagnetic simulation", *IEEE Trans. Magnetics*, vol. 42, no. 4, pp. 647-650, 2006.

[13] A. Manzin and O. Bottauscio, "Element-free Galerkin method for the analysis of electromagnetic-wave scattering", *IEEE Trans. Magnetics*, vol. 44, no. 6, pp. 1366-1369, 2008.

[14] D. S. Junior,"Numerical modelling of electromagnetic wave propagation by meshless local Petrov-Galerkin Formulations", CEMS, vol.50, no.2, pp.97-114, 2009.

[15] G. Liu, Mesh Free Methods: Moving Beyond the Finite Element Method, CRC Press, 2nd Edition 2009.

[16] A. Peterson, S. Ray, and R. Mittra, Computational Methods for Electromagnetics, IEEE Press, 1998, Sect. 8.8.

[17] S. N. Atluri and S. Shen, "The Meshless Local Petrov-Galerkin Method: A simple & less-costly alternative to the finite-element and boundary element methods", CMES, vol. 3, no 1, pp 11-51, 2002.

[18] Q.Liu, S. Shen, Z. Han, and S. Atluri, "Application of meshless local Petrov-Galerkin (MLPG) to problems with singularities, and material discontinuities, in 3-D elasaticity", CMES, vol.4, no5, pp.571-585,2003.

[19] R. W. P. King, Tables of Antenna Characteristics. New York: IFI/Plenum, 1971.